

UNTARGETED NMR-BASED METABOLOMICS ANALYSIS OF KIDNEY ALLOGRAFT PERFUSATES IDENTIFIES A SIGNATURE OF DELAYED GRAFT FUNCTION

A. Cirillo¹, M. Vandermeulen^{2,3}, P. Erpicum^{3,4}, T. Pinto Coelho³, N. Meurisse², O. Detry^{2,3}, F. Jouret^{3,4} et P. de Tullio¹

¹*Clinical Metabolomics Group, Center for Interdisciplinary Research On Medicines (CIRM), University of Liege, Liege, Belgium*

²*Department of Abdominal Surgery and Transplantation, CHU de Liege, University of Liege, Liege, Belgium*

³*Groupe Interdisciplinaire de Genoproteomique Appliquee (GIGA), Metabolism and Cardiovascular Sciences, University of Liege, Liege, Belgium*

⁴*Division of Nephrology, CHU de Liege, University of Liege, Liege, Belgium*

KEYWORDS : Metabolomics ; Kidney transplantation ; Delayed graft function ; NMR ; Perfusate

ABSTRACT

Introduction. Kidney transplantation (KTx) necessarily conveys an ischemia/reperfusion (I/R) process, which impacts on allograft outcomes. Delayed graft function (DGF) is defined as a non-decrease of serum creatinine by at least 10% daily on 3 consecutive days during the first 7 days post-KTx. DGF significantly conditions both short- and long-term graft outcomes. Still there is a lack of DGF predictive biomarkers.

Objectives. This study aimed to explore the potential of kidney graft perfusate metabolomics to predict DGF occurrence.

Methods. 49 human perfusates from grafts categorized upon donor type [donation after brain death (DBD)/donation after circulatory death (DCD)] and DGF occurrence and 19 perfusates from a murine model classified upon death type (DBD/DCD) were collected and analyzed by NMR-based metabolomics.

Results. The multivariate analysis of the murine data highlighted significant differences between perfusate metabolomes of DBD *versus* DCD. These differences were similarly observed in the human perfusates. After correcting for the type of donor, multivariate analysis of human data demonstrated a metabolomics signature that could be correlated with DGF occurrence.

Conclusions. The metabolome of kidney grafts is influenced by the donor's type in both human and pre-clinical studies and could be correlated with DGF in the human DBD cohort. Thus, metabolomic analysis of perfusate applied prior to KTx may represent a new predictive tool for clinicians in a more personalized management of DGF. Moreover, our data paves the way to better understand the impact of donor's types on the biochemical events occurring between death and the hypothermic storage.

1. Introduction

Kidney transplantation (KTx) currently represents the best treatment for patients with end-stage renal disease. Even if 90,000 KTx are performed each year worldwide, kidney transplantation outcome highly depends on graft quality before transplantation and, at present, no reliable tools exist to assess it. In clinical practice, a list of standard classification criteria (SCD) was redacted to guarantee graft quality, including kidney procured in donation after brain death (DBD) conditions (Metzger et al., 2003; Wang et al., 2020). The increasing gap between demand and supply for KTx has led to the use of suboptimal organ donors, such as donation after circulatory death (DCD) and extended criteria donors (ECDs) (Cooper et al., 2004; Koffman & Gambaro, 2003). However, kidneys coming from these donors (ECDs excluded) are exposed to a supplementary warm ischemia at procurement leading to higher risk of delayed graft function (DGF) and subsequently poorer graft outcomes (Jouret et al., 2016; Khbouz et al., 2022; Ponticelli, 2014; Salvadori et al., 2015; Wong et al., 2017). DGF is a pathological condition, often resulting from ischemic damage and defined as a non-decrease of serum creatinine by at least 10% daily on 3 consecutive days during the first 7 days post-KTx (Aydin et al., 2012). Aside from early complications following KTx, the occurrence of DGF in transplanted patients translates in lower graft function and worse short- and long-term outcomes (Bahl et al., 2019; Ponticelli et al., 2022). This clinical complication currently impacting approximately 25–30% of transplant recipients (Mannon, 2018) is associated to several donor-related factors including, among others, donor type (DCD at higher risk compared to DBD) and duration of warm and cold ischemia times (WIT/CIT) (Ponticelli et al., 2022). In way to minimize the risks related to ischemic damage, the usage of a cold preservation solution to be flushed in the organ, can minimize these events by decreasing metabolism and slowing the process leading to IRI (Peng et al., 2019). In recent studies, the use of IGL-1 (Institute Georges Lopez-1, France) cold storage solution has led to the reduction of DGF incidence (Badet et al., 2005). However, independently of the types of donors, reliable tools are needed to assess the quality of the graft after procurement and/or to better prevent DGF in clinical practice (Reese et al., 2021). In this context, metabolomics-based approach is particularly suited by placing itself as a solution tool adapted to personalized medicine setting for patient's treatment and follow-up (Ashrafian et al., 2021; Jacob et al., 2019; Letertre et al., 2021). This study hypostatized that perfusate solutions represent useful—still poorly explored—biofluids that could inform on what happened to the graft during its cold ischemic period, thereby providing the clinicians with informative data concerning the quality of the graft. Thus, using a Nuclear Magnetic Resonance (NMR)-based untargeted approach, this study aimed to analyze kidney perfusate solutions obtained just before transplantation in search of a metabolomic signature that could predict DGF occurrence in transplant patients. For this purpose, we had access to two types of perfusate samples, one from a human cohort and the other one from an animal model simulating the donor's type of donation. The parallel use of a human and experimental samples could enable us to explore two main points: (1) the biochemical events occurring between death and hypothermic storage of kidneys related to donor type; (2) the differences in metabolomics content between different donor types.

The final goals of this pilot study were (1) to demonstrate the value of perfusate metabolomic analysis in KTx; (2) to evaluate the impact of donor type on the graft metabolome during the cold ischemia period and (3) to generate a metabolomics model that could be useful as a predictive tool for DGF occurrence.

2. Materials and methods

2.1 WIT AND CIT

In this study, kidney transplantation events were described using the terms: warm ischemia time1 (WIT1), cold ischemia time (CIT), and warm ischemia time2 (WIT2).

WIT1 was measured as the period between the circulatory arrest and the cold perfusion of the kidneys. CIT was defined as the period between the initiation of the cold flush until the removal of the graft from the cold storage to be transplanted in the recipient. WIT2 was defined as the time between removal from cold storage to graft reperfusion in the recipient (suture time).

2.2 SURGICAL MODELS OF KIDNEY GRAFT PROCUREMENTS IN THE RAT

This experimental model has been essentially developed to mimic the different types of kidney graft donors. After induction of anesthesia (Isoflurane 2% in O₂ 2 l/min), a tracheotomy was performed to ensure optimal ventilation using a weight-based autoregulated rodent ventilator (PhysioSuite—KentScientific, Torrington, Connecticut, USA). Arterial and venous catheters (Polyurethane 0.43 × 0.69 m) were placed in the femoral vessels to allow continuous monitoring of intra-arterial pressure (Picco Monitoring Kit and BP-100; CWE inc, Ardmore, Oklahoma, USA) and to have a venous access for intraoperative fluid injection, respectively (Ethic agreement code: 2147).

2.2.1 DBD MODEL

In the DBD group (n = 9), brain death was induced under general anesthesia as previously described by Saat et al. (2016). In summary, after front lateral trepanation, a Fogarty balloon catheter (Edwards Lifesciences, Irvine, California, USA) was introduced and slowly inflated (100 µL/min for 4 min) into the extradural space. Brain death was confirmed by the absence of corneal and pupillary reflexes, the onset of a hypertensive peak followed by major hypotension and a 60 s apnea test as described (Esmailzadeh et al., 2020). The rats were maintained in a brain-death state for 6 h. The mean arterial pressure (MAP) was maintained above 60 mm Hg after induction of brain death by intravenous administration of normal saline (1 mL/h) and norepinephrine (1 mg/mL, Aguetant, Lyon, France) (5–15 µg/h) in case the administration of a 1 mL bolus of normal saline would not maintain MAP above 60 mmHg. Then, all animals received a continuous infusion of 1 mL/h of normal saline using an electric syringe pump (Becton Dickinson, Franklin Lakes, New Jersey, USA), previously warmed to body temperature, to compensate for insensible losses. The body temperature was maintained at

38 °C with a rectal probe-controlled temperature pad connected to the ventilator (PhysioSuite—KentScientific, Torrington, Connecticut, USA).

2.2.2 DCD MODEL

In the DCD group (n = 10), all animals received 1 mL normal saline/h, previously warmed to body temperature, to compensate for insensible losses. After 6 h of mechanical ventilation in a previously tracheostomized rat maintained under general anesthesia, circulatory arrest was induced by an intravenous injection of KCl (150 mg/kg) as previously described in rodent DCD models (Soussi et al., 2019). Circulatory arrest was defined upon cessation of aortic pulsatility and a fall in MAP below 25 mmHg.

2.2.3 KIDNEY PROCUREMENT AND PERFUSATE COLLECTION

After induction of circulatory (DCD group) or brain death (DBD group), a laparotomy was performed to remove the kidneys. Both kidneys were flushed with IGL-1 organ preservation solution through the aorta and then stored immersed in IGL-1 at 4 °C for 14 h, as a model of clinical CIT (left kidney). After 14 h of CIT, a second cold IGL-1 flush was made through the renal artery to collect the perfusate, defined as the first 2 mL of effluent evacuated from the renal vein. The perfusate was then stored at –80 °C until metabolomic analyses (9 DBD and 10 DCD perfusates).

2.3 CLINICAL KIDNEY TRANSPLANTATION

Informed consent was obtained from all KTx recipients included in the study (Ethics agreement: B707201524484). Clinical data about donor, graft and recipient were collected. Kidney donor risk index (KDRI) and kidney donor profile index (KDPI) were calculated based on donor and transplant factors (Rao et al., 2009).

Human kidney grafts procured from DBD or DCD donors were cold flushed during the procurement with IGL-1. All kidney grafts were preserved with classical static cold storage at 4 °C during variable CIT, according to the clinical situation, and were allocated to a given recipient by Eurotransplant. After preparation of the renal vessels before KTx on the back-table, the kidney grafts were flushed through the renal artery with 1 L of IGL1 solution. The first 10 mL of liquid exiting the renal vein during the flush were collected for metabolomics analysis and constituted the “perfusate”. A total of 49 perfusate samples were used in this study; 36 from DBD and 13 from DCD donors. Prior to DBD and DCD classification, samples were categorized based on donor criteria classification including SDC (n = 40) and ECD (n = 9). Among these 9 ECD donors, 7 were DBD and 2 were DCD. Concerning the post-transplantation status, 7 ECD donors experienced DGF, while 2 were classified as noDGF.

2.4 ¹H-NMR METABOLOMICS

All samples were recorded at 298 K on a Bruker Avance HD spectrometer (Bruker, Billerica, USA) operating at 700.17 MHz for the proton signal acquisition. The instrument was equipped with a TCI 5-mm cryoprobe with a Z-gradient. Maleic acid was used as the internal standard for quantification and trimethylsilyl-3-propionic acid-d4 (TMSP) for the zero for the zero calibration. An aliquot of

200 μL of perfusate samples was supplemented with 50 μL of deuterated phosphate buffer (DPB, pH 7.4), 25 μL of a 35 mM solution of maleic acid and 2 μL of a 10 mg/mL TMSP D₂O solution. ¹H-NMR spectra were acquired using a 1D NOESY sequence with presaturation. The Noesy presat experiment used a RD-90°-T1-90°-Tm-90°-acquire sequence with a relaxation delay of 4 s, a mixing time (Tm) of 10 ms and a fixed T1 delay of 4 μs . Water suppression pulse was placed during the relaxation delay (RD). The number of transients is 64 (64 K data points). The data were processed with the Bruker Topspin 4.0.8 software (Bruker BioSpin, Billerica, USA) with a standard parameter set. Phase and baseline corrections were performed manually over the entire range of the spectra and the δ scale was calibrated to 0 ppm using the internal standard TMSP.

2.5 MULTIVARIATE ANALYSIS

Once the spectra obtained, identification and quantification of metabolites were performed through Chenomx profiler 9.0 (Chenomx Inc., Edmonton, AB, Canada). The profiled spectra were used to generate a concentration table that was imported in BioStatFlow webtool (biostatflow.org) for multivariate statistical analysis. Autoscaling normalization was applied to concentration table. Principal component analysis (PCA) was used for looking at outliers and cluster between samples. An orthogonal signal correction-PLS model (OSC-PLS) was performed as discriminant model and its quality was determined by the predictability calculated based on the fraction correctly predicted in one-seventh cross-validation (Q^2). Permutation tests were performed to validate models. Metaboanalyst (www.metaboanalyst.ca) was used for generating multivariate receiver operating characteristic (ROC) curves and confusion matrix to assess the robustness of the models. ROC curves were performed by using PLS-DA models as classification method and univariate AUROC as feature ranking method with two latent variables. Confusion matrix was used for calculating model sensitivity and specificity.

2.6 UNIVARIATE AND PATHWAYS ANALYSIS

Univariate analysis was made using GraphPad Prism version 9.4.1 (GraphPad Software, La Jolla, CA, www.graphpad.com). Mann-Whitney U test was performed for comparisons between two groups. No correction was applied to Mann-Whitney U tests. The detailed analysis of the metabolic pathways was performed by Metaboanalyst (www.metaboanalyst.ca) using the metabolomic set enrichment analysis (MSEA) tool by using the high-quality SMPDB metabolic pathways as the backend knowledgebase.

3. Results

3.1 STUDY POPULATION

A preliminary statistical analysis was conducted on the cohort considering the donor criteria classification including SDC and ECD, which showed no confounding factors. Donor characteristics categorized by the type of death event are presented in Table 1.

Table 1. Clinical characteristics of donors

	DBD (N=36)	DCD (N=13)	Total (N=49)	p-value
Sex				0.233
F	15 (41.7%)	3 (23.1%)	18 (36.7%)	
M	21 (58.3%)	10 (76.9%)	31 (63.3%)	
Age				0.774
Mean (SD)	45.361 (13.495)	46.692 (16.311)	45.714 (14.130)	
Range	19.000 - 68.000	18.000 - 67.000	18.000 - 68.000	
BMI				0.348
N-Miss	0	1	1	
Mean (SD)	25.739 (4.159)	24.502 (3.016)	25.429 (3.912)	
Range	17.700 - 35.900	20.000 - 30.000	17.700 - 35.900	
Serum creat (mg/dl)				0.277
Mean (SD)	0.789 (0.253)	0.703 (0.202)	0.766 (0.242)	
Range	0.310 - 1.400	0.430 - 1.120	0.310 - 1.400	
Weight				0.948
N-Miss	0	1	1	
Mean (SD)	77.111 (13.509)	76.833 (9.437)	77.042 (12.521)	
Range	47.000 - 110.000	65.000 - 94.000	47.000 - 110.000	
Diabetes				0.648
N-Miss	5 (13.9%)	1 (7.7%)	6 (12.2%)	
No	30 (83.3%)	11 (84.6%)	41 (83.7%)	
Yes	1 (2.8%)	1 (7.7%)	2 (4.1%)	
Hypertension				0.831

N-Miss	5 (13.9%)	1 (7.7%)	6 (12.2%)	
No	24 (66.7%)	9 (69.2%)	33 (67.3%)	
Yes	7 (19.4%)	3 (23.1%)	10 (20.4%)	
Cause of death				0.008
Anoxia	8 (22.2%)	9 (69.2%)	17 (34.7%)	
Cerebral hemor	19 (52.8%)	2 (15.4%)	21 (42.9%)	
Trauma	9 (25.0%)	2 (15.4%)	11 (22.4%)	
KDPI %				0.386
N-Miss	1	1	2	
Mean (SD)	39.361 (27.234)	47.308 (30.398)	41.469 (28.007)	
Range	0.000 - 92.000	0.000 - 89.000	0.000 - 92.000	
KDRI				0.228
N-Miss	1	1	2	
Mean (SD)	0.937 (0.277)	1.053 (0.302)	0.967 (0.285)	
Range	0.570 - 1.660	0.640 - 1.540	0.570 - 1.660	

BMI body mass index, *Serum creat* serum creatinine mg/dl, *KDPI* kidney donor profile index (%), *KDRI* kidney donor risk index

Statistical analysis on recipient data (DGF = 19; noDGF = 30) showed no correlation between DGF status and related clinical data (Table 2).

Table 2. Clinical characteristics of receivers based on graft outcome DGF or noDGF

	DGF (N=19)	noDGF (N=30)	Total (N=49)	p-value
Sex				0.326
Female	9 (47.4%)	10 (33.3%)	19 (38.8%)	
Male	10 (52.6%)	20 (66.7%)	30 (61.2%)	
Age				0.606
Mean (SD)	59.000 (12.396)	57.000 (13.562)	57.776 (13.028)	
Range	28.000 - 72.000	22.000 - 73.000	22.000 - 73.000	
CIT				0.377
Mean (SD)	604.158 (281.886)	677.867 (281.889)	649.286 (281.286)	
Range	207.000 - 1069.000	189.000 - 1300.000	189.000 - 1300.000	

WIT1				0.732
Mean (SD)	2.105 (3.710)	2.533 (4.531)	2.367 (4.197)	
Range	0.000 - 11.000	0.000 - 16.000	0.000 - 16.000	
WIT2				0.363
Mean (SD)	37.316 (12.352)	40.000 (8.154)	38.959 (9.956)	
Range	21.000 - 54.000	19.000 - 55.000	19.000 - 55.000	

CIT cold ischemia time, *WIT1* warm ischemia time, *WIT2* warm ischemia time 2

3.2 PRELIMINARY ANALYSIS ON IGL-1 MATRIX

A preliminary metabolomics analysis allowed to spot a series of peaks coming from IGL-1 matrix represented by lactobionic acid, adenosine, raffinose, and glutathione signals (S2, S3, S4 and S5). These peaks were identified, quantified, and excluded from following analysis on perfusate samples.

3.3 PERFUSATE METABOLOMES IN RAT MODELS: DIFFERENCES BETWEEN DBD AND DCD DONORS

Nineteen perfusate samples were included in the analysis. DBD and DCD kidney donor conditions were mimed in 9 and 10 rats, respectively. After exclusion from statistical analysis of matrix-linked peaks, 44 quantified metabolites that are belonging to the kidney metabolome were used for multivariate statistical models. Supervised statistical investigations using OSC-PLS highlighted a significant discrimination between DBD donor type versus DCD donor type ($Q^2 = 0.621$); the model was validated through a permutation test (p -value = 0.0393), confirming the absence of overfitting (Fig. 1).

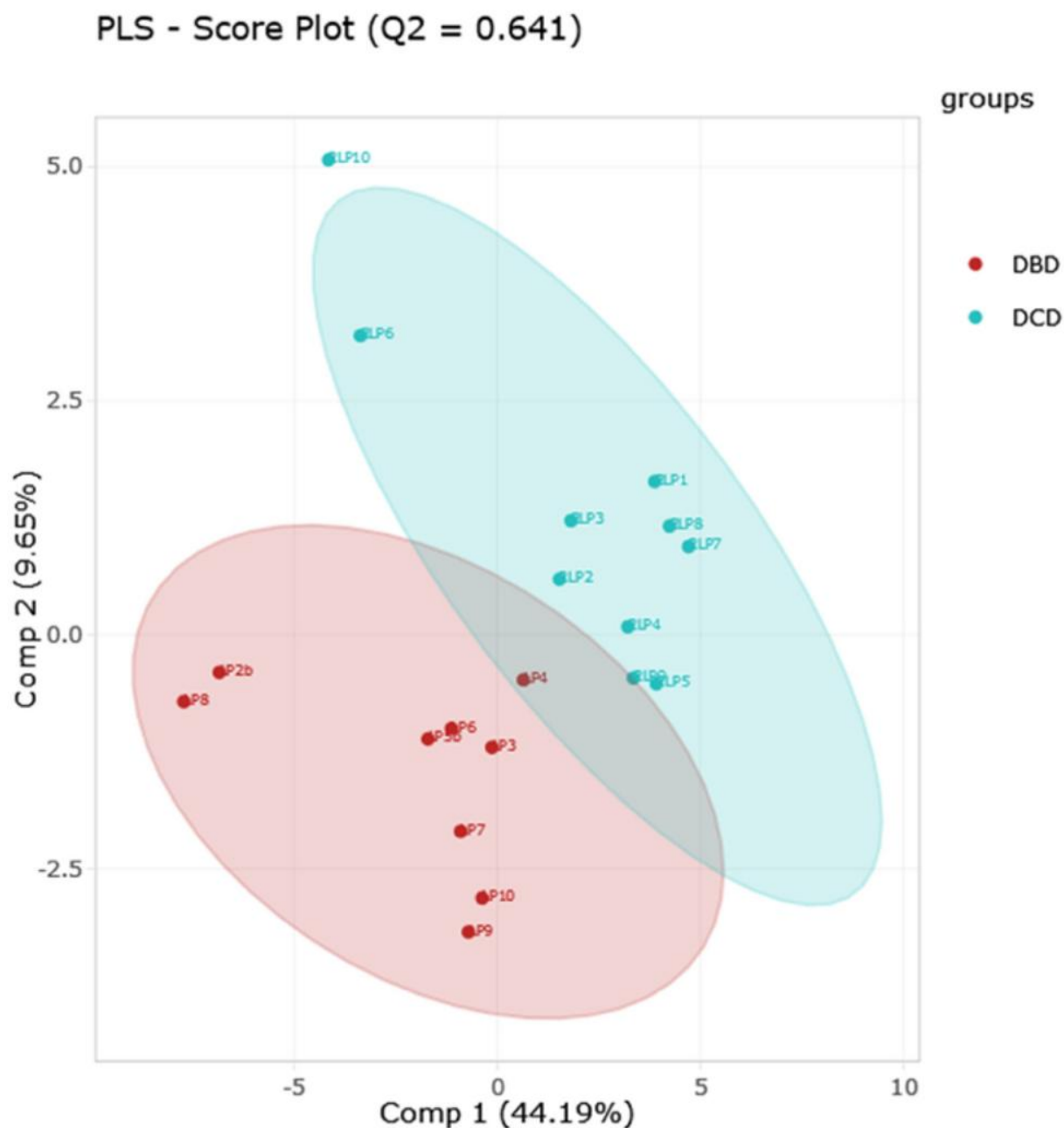


Fig. 1. OSC-PLS model of rat model showing variation of metabolomics profile according to donor type (Q2 = 0.641; cross validation p-value = 0.0393; n total = 19)

A loading-plot was generated in way to underline all the metabolites responsible for the discrimination of groups according to donor type. Based on the results of multivariate models, univariate statistical analysis revealed that the concentrations of 7 metabolites were increased in DCD status compared to DBD status, including 2-hydroxyisovalerate, 2-octenoate, 2-oxocaproate, 3-hydroxyisovalerate, alloisoleucine, creatine phosphate, lysine, o-phosphoethanolamine, taurine and valine (Fig. 2).

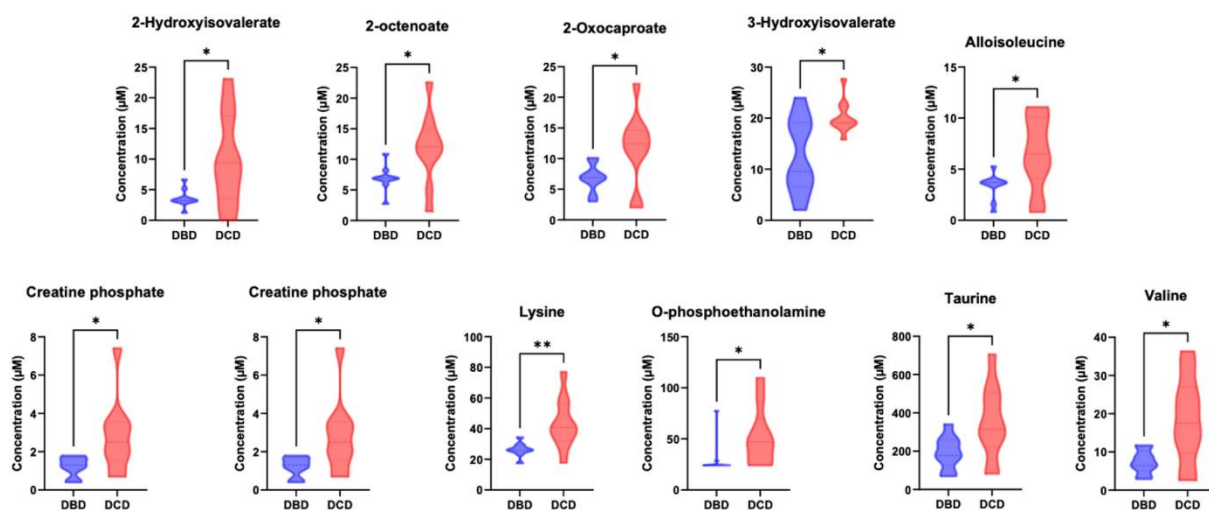


Fig. 2. Violin-plots of significant metabolites in rat perfusate of DBD (n = 9) versus DCD (n = 10). Mann-Whitney U test was used. (* < 0.05; ** < 0.001)

3.4 PERFUSATE METABOLOMES IN HUMAN COHORT: DIFFERENCES BETWEEN DBD AND DCD DONORS

Forty-nine human perfusate samples were included in the analysis. Multivariate and univariate analyses based on donor criteria (SCD/ECD) indicated no significant statistical impact. Once this confounding factor was excluded, another analysis was conducted on the samples categorized by donor type (DBD = 36; DCD = 13). A total of 54 metabolites were identified independently from IGL-1 matrix and quantified (S1, S2, S3, S4 and S5). Multivariate statistical analysis was performed by generating a discriminant OSC-PLS model ($Q^2 = 0.540$); a permutation test (p-value = 0.02192) was performed by validating the model obtained (Fig. 3).

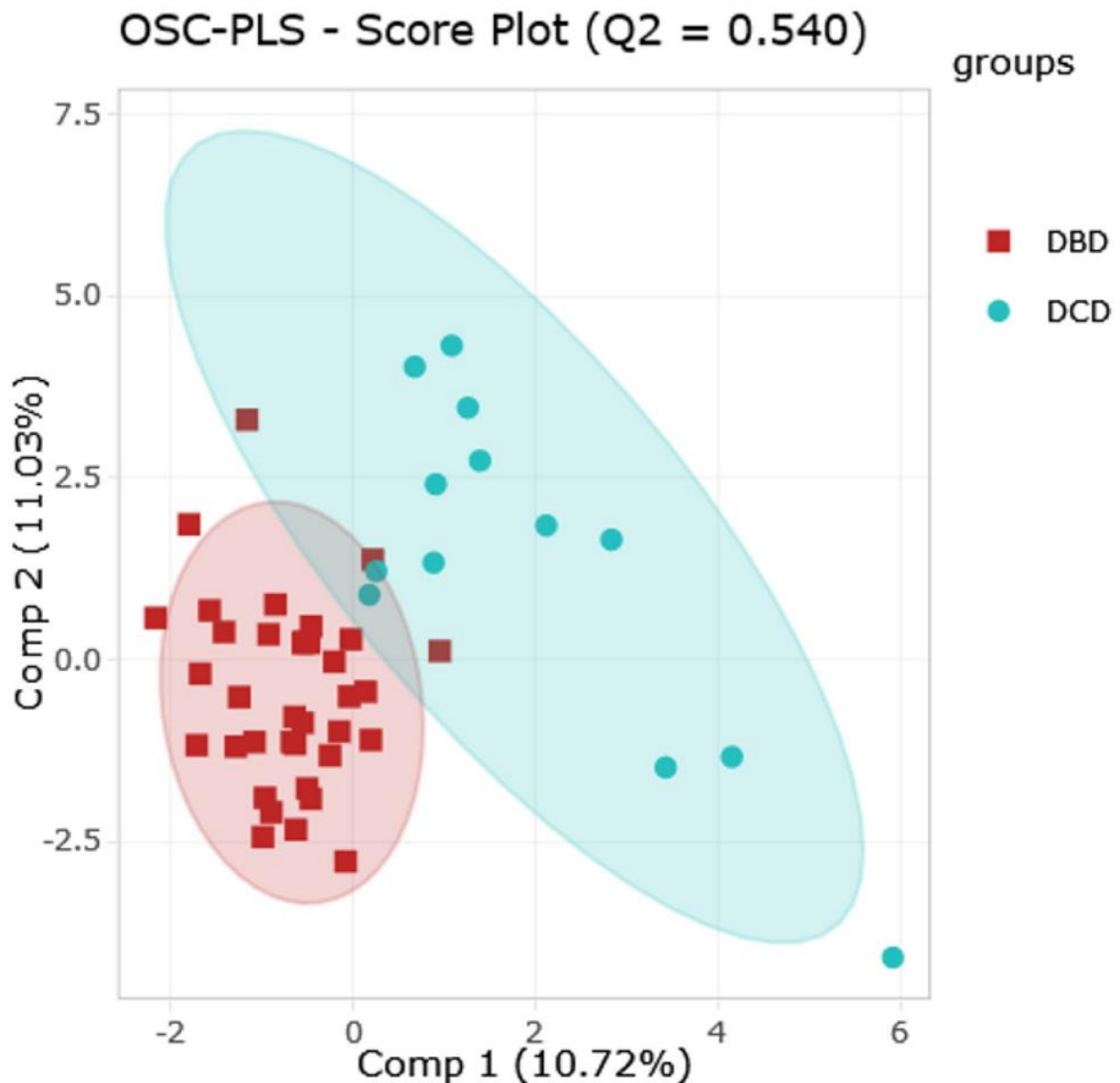


Fig. 3. Multivariate analysis based on donor types in human model (n total = 39). OSC-PLS score plot showing a separation between DBD versus DCD donor (Q2 = 0.540; cross validation p-value = 0.02192)

The metabolites relevant for discrimination between groups in multivariate models were used to perform univariate statistical analysis. Mann–Whitney U tests highlighted 17 metabolites significantly differing between donor types. Twelve metabolites were increased in DCD donor group (e.g., valine and cystine) while five were decreased compared to DBD group (e.g., lactate and trimethylamine-*N*-oxide) (Fig. 4).

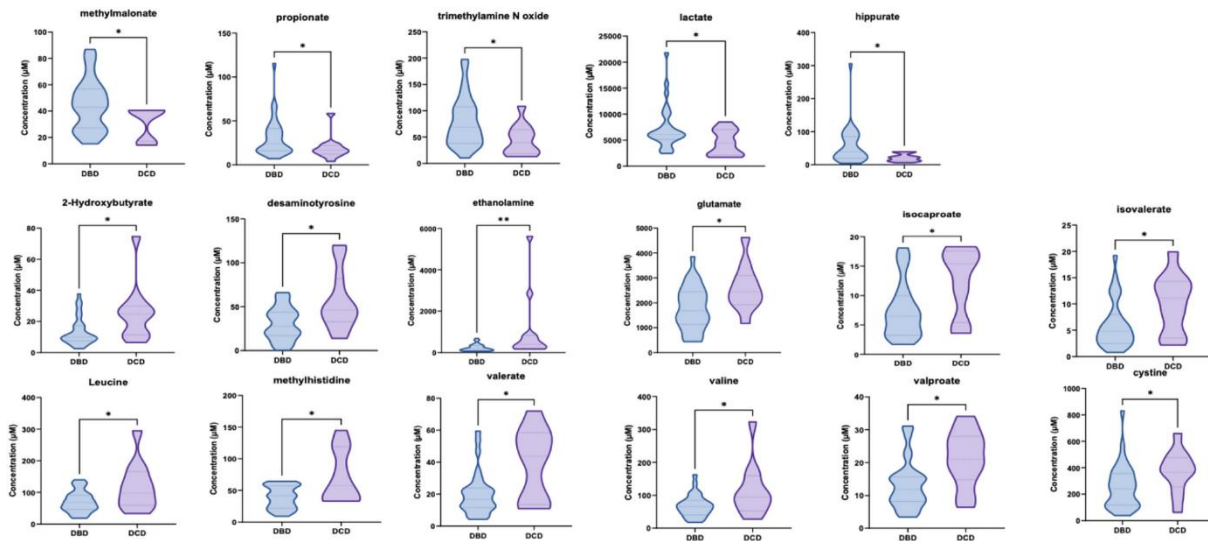


Fig. 4. Violin-plots for metabolites of human cohort with significant variation according to DBD (n = 36) versus DCD (n = 13). Comparison between groups was made by using Mann–Whitney U test. (* < 0.05; ** < 0.001)

3.5 INSIGHTS INTO COMMON METABOLIC PATHWAYS IN HUMAN AND RAT PERFUSATES

By comparing the significant metabolites obtained in the two models, it was possible to spot some common features such as valine and isoleucine. In way to better investigate the biochemical events occurring during the hypothermic storage of kidney, a pathway analysis was conducted. MSEA analysis led to the identification of several pathways significantly affected by donor type (Fig. 5a–b). The most relevant cascades were, in both models, represented by valine/leucine/isoleucine biosynthesis and degradation, aminoacyl-t-RNA biosynthesis, alanine/aspartate/ glutamate metabolism and glycerophospholipid metabolism.

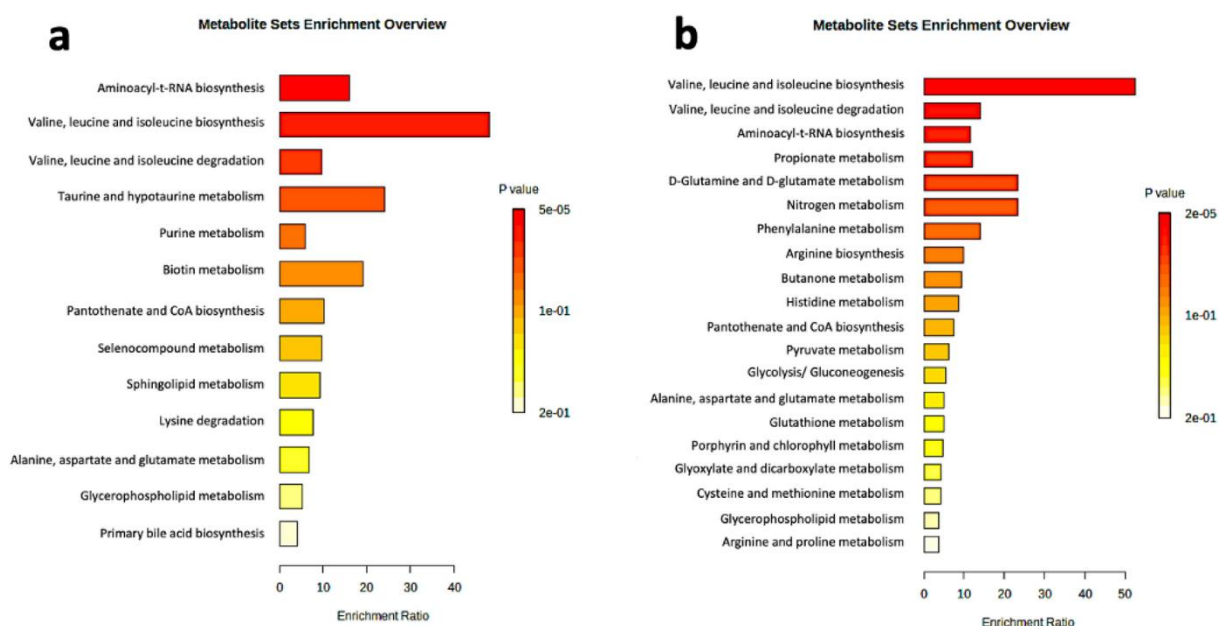


Fig. 5. Comparison of MSEA analysis in human and rat models showed common biochemical pathways

involved in the process of DBD and DCD; **a** MSEA analysis of human cohort based on significant metabolites related to donor type; **b** MSEA analysis of rat model for DBD versus DCD groups

3.6 CORRELATION OF ¹H-NMR-BASED HUMAN PERFUSATE METABOLOME WITH DGF INCIDENCE POST-KTX

By considering DGF outcome as factor (DGF = 19; noDGF = 30), OSC-PLS model was used as a discriminant analysis ($Q^2 = 0.370$; P-value = 0.4387). Moreover, a multivariate receiver operating characteristics (ROC) curve was generated by using the ratios of 54 identified metabolites (73 variables; AUC = 0.777; predictive accuracy = 71.6%) in way to evaluate the performance of our model through automated feature selection (Fig. 6a–b). Univariate analysis showed 12 metabolites being significantly increased in noDGF status (such as cystine, leucine, alanine ...), unlike carnosine (Fig. 7).

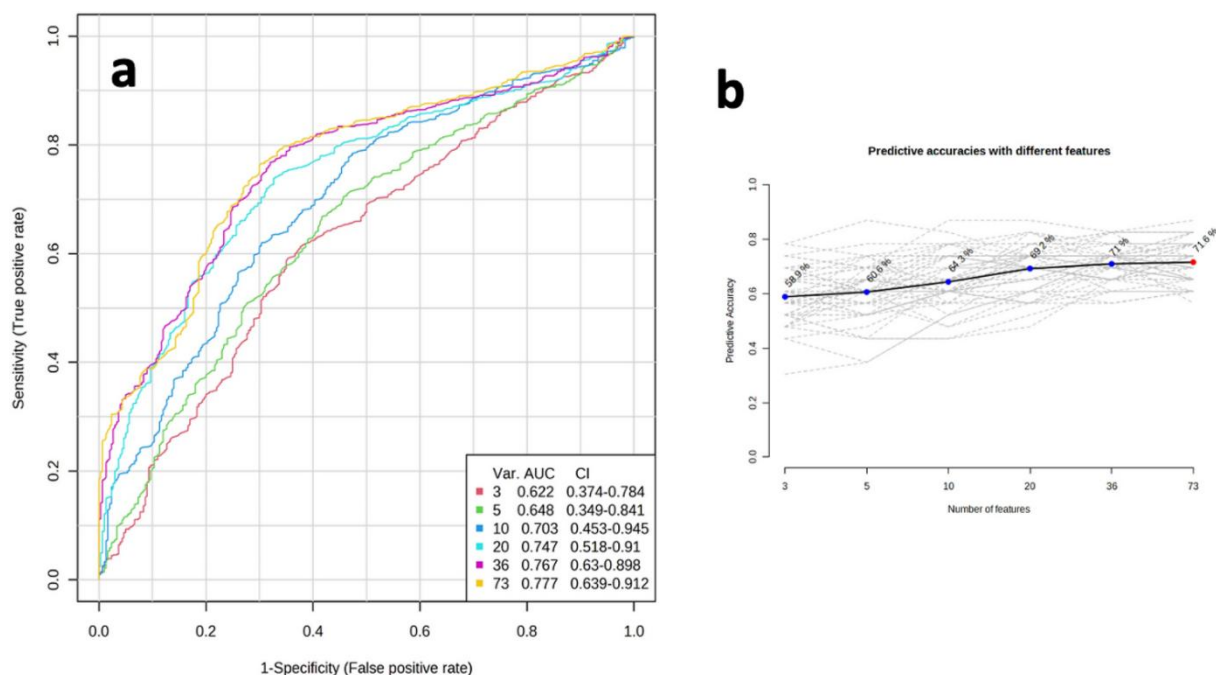


Fig. 6. Predictive models of DGF occurrence in the human cohort: **a** multivariate ROC curve based on DGF versus noDGF analysis with automated selection of ratio features showed an AUC = 0.777 by considering 73 variables; **b** plot showing the predictive accuracy with different features by reaching a value 71.6% with 73 variables

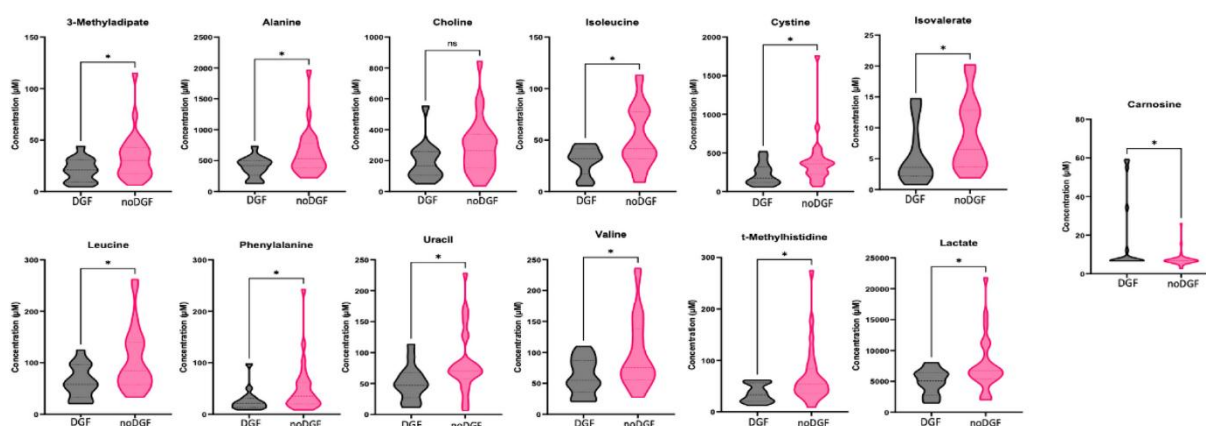


Fig. 7. Violin plots of significant metabolites according to DGF (n = 19) versus noDGF (n = 30) in human model. Comparison between groups was made by using Mann–Whitney U test. (* < 0.05; ** < 0.001)

In the perfusates from DBD kidneys, 36 perfusate samples were used for the univariate and multivariate statistical analyses by using DGF status as discriminant factor. A discriminant OSC-PLS model was generated ($Q^2 = 0.747$; p value = 0.2642) to look at the separation between the noDGF and the pathological status (Fig. 8a). Furthermore, the multivariate ROC curve showed a good performance by using the ratios of the 54 identified metabolites generated through Metaboanalyst algorithm (73 variables; AUC = 0.917; predictive accuracy = 83%) (Fig. 8b). A confusion matrix was additionally performed to cross-validate the model by highlighting all the automated selected ratio features used by the algorithm (Fig. 8c).

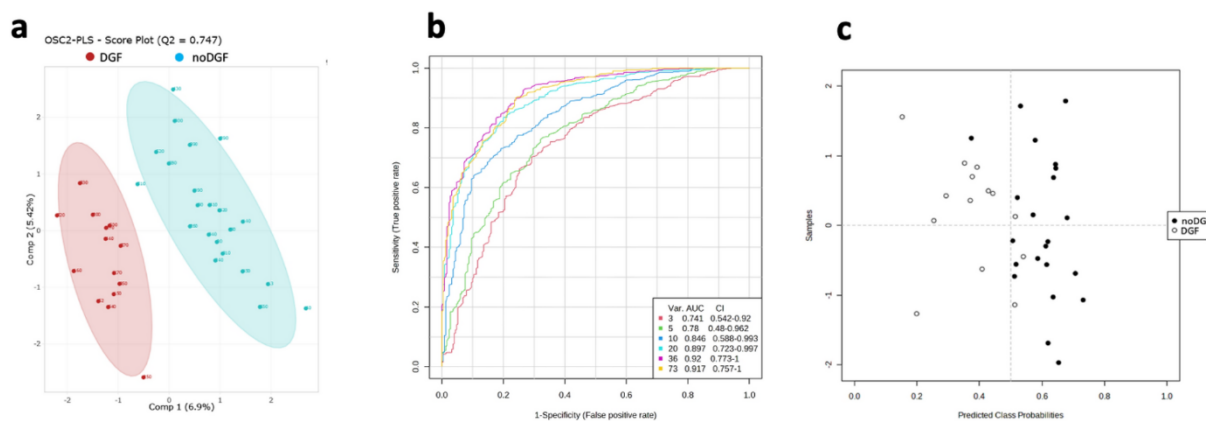


Fig. 8. Prediction of DGF kidney outcome in DBD group (human cohort); **a** OSC-PLS score plot show a separation between groups ($Q^2 = 0.747$; p-value = 0.2642); **b** multivariate ROC curve of DBD group based on DGF versus noDGF analysis with automated selection of ratio features showed an AUC = 0.917 by considering 73 variables; **c** confusion matrix was generated to evaluate model performance

Mann–Whitney t-tests highlighted 15 metabolites being significantly increased (e.g., lactate, alloisoleucine, isovalerate...) and ethylmalonate and carnosine being decreased in noDGF condition in comparison to DGF condition (Fig. 9). To identify biologically meaningful patterns a MSEA analysis was done showing that methylhistine/beta-alanine metabolism and valine, leucine and isoleucine degradation are the pathways more significantly impacted.

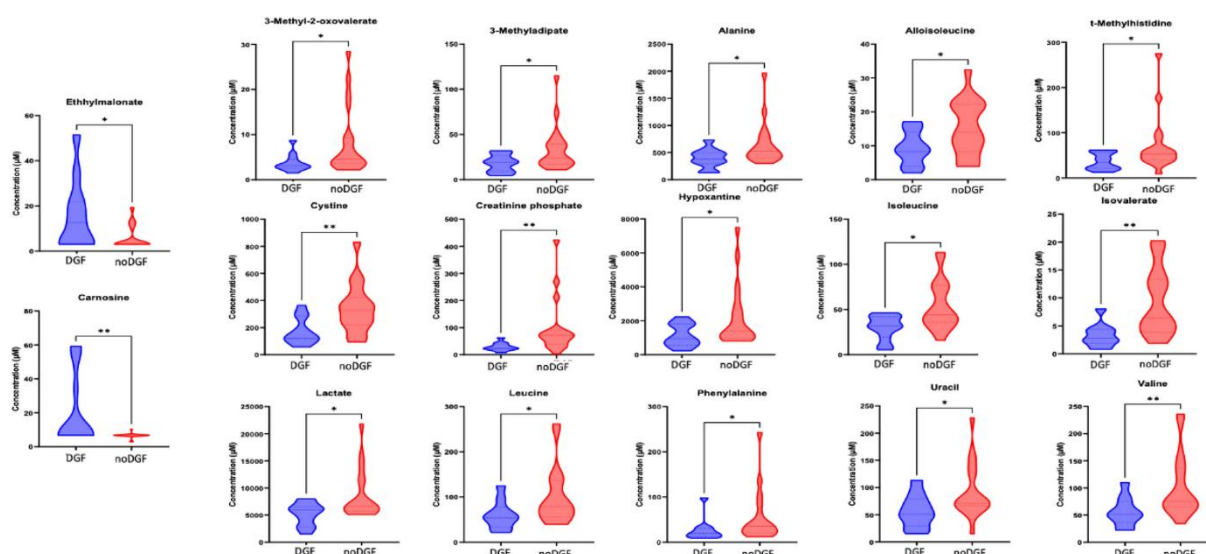


Fig. 9. Violin-plots of significant metabolites of DBD subgroup according to the analysis DGF (n = 14) versus noDGF (n = 22) in human model. Mann–Whitney U test was used for comparison

A total of 13 perfusates from DCD donors were used for statistical analysis by using graft outcome as discriminant factor (data not shown). The low number of samples for each group (DGF = 5; noDGF = 8) highlighted the over fitting of the model and a consequent poor performance ($Q^2 = 0.7333$; P-value = 0.4995). Univariate statistical analysis by using Mann–Whitney t-test showed only one metabolite significant for the discrimination of the two groups: creatinine phosphate.

4. Discussion

DGF represents one major obstacle in allograft survival (Siedlecki et al., 2011). Still, no single biomarker or a biochemical signature of graft quality and DGF prediction has been found and used routinely in clinical practice. The metabolomics approach has already been applied in several studies related to renal pathology and dysfunction on urine or plasma samples, leading to the discovery of metabolites linked to pathological status (Humphries et al., 2023; Iwamoto et al., 2022; Wishart, 2006). Its non-invasive nature makes this approach have advantages over biopsy in the context of graft status monitoring. Thus, several metabolomic studies of renal perfusate are described in the literature with particular emphasis on the correlation between perfusion time and metabolic content. (Bon et al., 2014; Faucher et al., 2022; Guy et al., 2015). In addition, other works have investigated perfusates of porcine models through NMR technique and have shown changes in metabolome's profiles of DCD donors between different perfusion strategies (Darius et al., 2020; Nath et al., 2017; Peng et al., 2019). However, at that time, no relevant metabolomic signature or predictive model was reported about the occurrence of DGF condition.

The first question to ask is whether there is a difference in the graft metabolome depending on the harvesting conditions (DCD or DBD). Using our pre-clinical experimental model, we were able to demonstrate that the metabolomes of the DCD and DBD groups were significantly different. Specifically, perfusate analysis revealed higher levels of seven metabolites, including lysine,

isoleucine, and valine, in DCD samples compared to DBD samples. In the human cohorts, these metabolic trends were confirmed with more than 17 metabolites levels that significantly differs according to the donor type. Some of these metabolites were common in both rat model and human study. More interestingly, several common biochemical pathways such as valine, leucine and isoleucine degradation/biosynthesis and aminoacyl-tRNA biosynthesis were also identified and could be correlated with some data in the literature. Thus, Hrydziuszko et al. previously observed the implication of these biochemical pathways in the DCD graft in the context of liver transplantation (Hrydziuszko et al., 2016). These similarities, albeit partial, between the metabolomic profiles of the experimental model and human samples demonstrated the value of the animal model for mimicking the graft according to the type of donor. Moreover, in the human study, lactate, trimethylamine-*N*-oxide (TMAO) and methylmalonate were also found to be significantly higher in DBD graft in comparison to DCD graft. Modulations in lactate levels could be explained by the major change in the metabolic oxidative process following brain death by underlying a change from aerobic to anaerobic metabolism in the graft (Novitzky et al., 1988; van Der Hoeven et al., 2003). Higher levels of TMAO, could be linked to a more important renal medullary damage due to ischemic events in DBD graft compared to DCD (Hauet et al., 2000; Robert et al., 2010). Differences in metabolic profiles related to donor types may also find an explanation in metabolic changes in the kidney due to the I/R process, as already reported in the literature (Jouret et al., 2016), and to the warm ischemia typical of DCD donors.

All these data showed that the biochemical processes that took place within the graft during the period of cold ischemia were different depending on the type of donor and need to be explored more in details. Furthermore, it could be expected that these metabolomic differences could be linked to the occurrence of DGF after transplantation and long-term outcomes in recipients. This shows that, in our view, each type of donor should be studied separately.

This was confirmed when we studied the correlation between the graft metabolome and the occurrence of DGF. Indeed, the results obtained using the data from the whole cohort (DBD and DCD donors together) showed a poor performance in predicting the post-transplantation graft outcome. While focusing our analysis on DBD-derived perfusates improved the quality of the predictive DGF occurrence model. Indeed, the multivariate ROC curve and the matrix of confusion obtained are quite relevant and compatible with a clinical predictive use for DGF occurrence demonstrating the interest of perfusate analysis for the recipients' follow-up.

Moreover, this approach led also to the identification of several biomarkers that differed in concentrations in the perfusates of DGF kidneys compared to noDGF kidneys. Alanine, isoleucine, leucine, valine and other branched chain amino acids were detected to be in significantly lower levels in DGF kidneys. These metabolites were released by the graft which can attest the sustained metabolic activity, ischemic damage, or both. Guy et al. previously observed raised concentrations of amino acids that may be linked to increased cellular breakdown in more ischemically damaged DGF kidneys (Guy et al., 2015). However, their results were based on the perfusate's analysis of DCD graft 45 min after perfusion with KPS-1 cold storage solution, which hampers direct comparison with our results. Otherwise, Carnosine and ethyl-malonate, were significantly increased in DGF kidneys.

The role of carnosine in kidney function has recently been investigated and shown a significantly lower urinary carnosine excretion in kidney transplant recipients compared to healthy group leading to higher risk of graft failure (Rodriguez-Niño et al., 2021). Potential mechanism of action of this metabolite included lowering of chronic low-grade inflammation, as demonstrated in animal models in which treatment through carnosine was associated with attenuation of I/R-induced renal dysfunction (Fujii et al., 2003; Kurata et al., 2006). Thus, the higher level of carnosine in the perfusate samples of DGF kidney could be correlated to a possible increase of I/R damage. Levels of ethylmalonate was increased in the more ischemically damaged DGF kidneys, which would suggest changes in normal function of tricarboxylic acid (TCA) cycle organic anions (OAs). The biological mechanism linking TCA cycle organic anions with kidney dysfunction is not fully understood, but some studies have reported the relationship of these biomarkers with kidney function (Geubelle et al., 2017; Gilissen et al., 2016; Lunyera et al., 2022). A more fundamental study using rat models of kidney transplantation would provide a better understanding of the role of metabolites and associated biochemical pathways in graft function during cold ischemia. This would also allow us to better understand the impact that these metabolic pathways could have on the occurrence of DGF.

Considering all these findings, we are also aware of the limitations of our present pilot study. Our findings need obviously to be validated and confirmed in human by studying a new cohort with an increased number of DCD patients. The development of a rat transplantation models could also be valuable, especially for a more fundamental study of the metabolic pathways implied in DGF events. Another limitation of our study is the lack of complete clinical data and of biofluids from the donors that could allow us to obtain a more complete view on graft and allow to refine and complete the data concerning the graft before transplant.

5. Conclusion

In KTx, a better understanding of graft quality and a better prediction of short-term renal function in the recipient patient are essential both to improve graft selection and to provide more precise, personalized patient management. By studying the fluid preserved in the graft obtained just before transplantation, we were able to identify, both in an animal model and in a human cohort, some differences in the kidney metabolome depending on the type of donor (DCD or DBD). These differences were directly associated with alterations in the metabolic pathways of the graft, potentially exerting additional influence on kidney function recovery post-KTx. In view of these results, it is obvious that DCD and DBD samples could be analyzed in separate models. Thus, we have demonstrated that using the perfusate sample in DBD donors could allow to predict the occurrence of DGF status prior to surgery and to identify a panel of metabolites that could be correlated to this status.

Our data paves the way to better understand the impact of donor's types on the biochemical events occurring between death and hypothermic storage and to correlate some metabolites of the storage liquid with the occurrence of DGF. This acquired knowledge may help clinicians in the elucidation of

the biochemical events occurring between death and transplantation per se to improve the process of organ procurement and reduce the discard rate.

Obviously, our preliminary results need to be confirmed on a validation cohort that could also include biofluid samples and complete clinical data from both donor and recipients. Moreover, the development of rat models of kidney transplantation from DCD or DBD donors as well as a better exploration of the identified biochemical pathways implied will also allow a better understanding of the ischemic events whose intricate interconnections that play a pivotal role in shaping the graft outcome.

SUPPLEMENTARY INFORMATION

The online version contains supplementary material available at <https://doi.org/10.1007/s11306-024-02106-1>.

AUTHOR CONTRIBUTIONS

VM, OD, NM, TPC: identified the patients and collected the samples. AC: samples and performed NMR analysis and multivariate/univariate statistics. PT and FJ: supervised the study. AC: wrote the first draft. PT, FJ, VM, TPC and PE: critically reviewed and revised the draft. All authors read and verified the manuscript.

FUNDING

AC, PE and PT are respectively a FRIA grantee, a Fellow and a research director of the Fonds de la Recherche Scientifique-FNRS. FJ received support from the University of Liège (Fonds Spéciaux à la Recherche, Fonds Léon Fredericq) and the FNRS (Research Credits 2016 and 2019). TPC received support from the University of Liege (Fonds Léon Fredericq) and from Société Francophone de Néphrologie, Dialyse et Transplantation (SFNDT). AC received support from the University of Liege (Fonds Léon Fredericq).

DATA AVAILABILITY

NMR data for study in RAW format is freely available in the MetaboLights repository with study identifier MTBLS9015 (www.ebi.ac.uk/metabolights/).

Declarations

COMPETING INTERESTS

The authors declare no competing interests.

ETHICAL APPROVAL

For the human cohort, ethical approval for the use of perfusate samples and associated metadata in this study was obtained from CHU of Liege (Ethic agreement code: B707201524484). For animal model, all applicable international, national, and/or institutional guidelines for the care and use of animals were followed (Ethic agreement code: 2147).

RESEARCH INVOLVING HUMAN AND ANIMAL RIGHTS

All procedures performed in studies involving human participants were in accordance with the ethical standards of the institutional and/or national research committee and with the 1964 Helsinki declaration and its later amendments or comparable ethical standards.

References

- Ashrafian, H., Sounderajah, V., Glen, R., Ebbels, T., Blaise, B. J., Kalra, D., Kultima, K., Spjuth, O., Tenori, L., Salek, R. M., Kale, N., Haug, K., Schober, D., Rocca-Serra, P., O'Donovan, C., Steinbeck, C., Cano, I., De Atauri, P., & Cascante, M. (2021). Metabolomics: The stethoscope for the twenty-first century. *Medical Principles and Practice*, 30(4), 301–310. <https://doi.org/10.1159/000513545>
- Aydin, Z., Mallat, M. J. K., Schaapherder, A. F. M., Van Zonneveld, A. J., Van Kooten, C., Rabelink, T. J., & De Fijter, J. W. (2012). Randomized trial of short-course high-dose erythropoietin in donation after cardiac death kidney transplant recipients. *American Journal of Transplantation*, 12(7), 1793–1800. <https://doi.org/10.1111/j.1600-6143.2012.04019.x>
- Badet, L., Petruzzo, P., Lefrancois, N., McGregor, B., Espa, M., Berthillot, C., Danjou, F., Contu, P., Aissa, A. H., Virieux, S. R., Colpart, J. J., & Martin, X. (2005). Kidney preservation with IGL-1 solution: A preliminary report. *Transplantation Proceedings*, 37(1), 308–311. <https://doi.org/10.1016/j.transproceed.2004.12.045>
- Bahl, D., Haddad, Z., Dato, A., & Qazi, Y. A. (2019). Delayed graft function in kidney transplantation. *Current Opinion in Organ Transplantation*, 24(1), 82–86. <https://doi.org/10.1097/MOT.00000000000000604>
- Bon, D., Claire, B., Thuillier, R., Hebrard, W., Boildieu, N., Celhay, O., Irani, J., Seguin, F., & Hauet, T. (2014). Analysis of perfusates during hypothermic machine perfusion by NMR spectroscopy: A potential tool for predicting kidney graft outcome. *Transplantation*, 97(8), 810–816. <https://doi.org/10.1097/TP.0000000000000046>
- Cooper, J. T., Chin, L. T., Krieger, N. R., Fernandez, L. A., Foley, D. P., Becker, Y. T., Odorico, J. S., Knechtle, S. J., Kalayoglu, M., Sollinger, H. W., & D'Alessandro, A. M. (2004). Donation after cardiac death: The University of Wisconsin experience with renal transplantation. *American Journal of Transplantation*, 4(9), 1490–1494. <https://doi.org/10.1111/j.1600-6143.2004.00531.x>

Darius, T., Vergauwen, M., Smith, T. B., Patel, K., Craps, J., Joris, V., Aydin, S., Ury, B., Buemi, A., De Meyer, M., Nath, J., Ludwig, C., Dessy, C., Many, M.-C., Gianello, P., & Mourad, M. (2020). Influence of different partial pressures of oxygen during continuous hypothermic machine perfusion in a pig kidney ischemia-reperfusion autotransplant model. *Transplantation*, 104(4), 731–743. <https://doi.org/10.1097/TP.0000000000003051>

Esmaeilzadeh, M., Sadeghi, M., Heissler, H. E., Galmbacher, R., Majlesara, A., Al-Afif, S., & Mehrabi, A. (2020). Experimental rat model for brain death induction and kidney transplantation. *Journal of Investigative Surgery*, 33(2), 141–146. <https://doi.org/10.1080/08941939.2018.1480677>

Faucher, Q., Alarcán, H., Sauvage, F.-L., Forestier, L., Miquelestorena-Standley, E., Nadal-Desbarats, L., Arnion, H., Venhard, J.-C., Brichart, N., Bruyere, F., Marquet, P., & Barin-Le Guellec, C. (2022). Perfusate metabolomics content and expression of tubular transporters during human kidney graft preservation by hypothermic machine perfusion. *Transplantation*, 106(9), 1831–1843. <https://doi.org/10.1097/TP.0000000000004129>

Fujii, T., Takaoka, M., Muraoka, T., Kurata, H., Tsuruoka, N., Ono, H., Kiso, Y., Tanaka, T., & Matsumura, Y. (2003). Preventive effect of l-carnosine on ischemia/reperfusion-induced acute renal failure in rats. *European Journal of Pharmacology*, 474(2–3), 261–267. [https://doi.org/10.1016/S0014-2999\(03\)02079-X](https://doi.org/10.1016/S0014-2999(03)02079-X)

Geubelle, P., Gilissen, J., Dilly, S., Poma, L., Dupuis, N., Laschet, C., Abboud, D., Inoue, A., Jouret, F., Pirotte, B., & Hanson, J. (2017). Identification and pharmacological characterization of succinate receptor agonists. *British Journal of Pharmacology*, 174(9), 796–808. <https://doi.org/10.1111/bph.13738>

Gilissen, J., Jouret, F., Pirotte, B., & Hanson, J. (2016). Insight into SUCNR1 (GPR91) structure and function. *Pharmacology & Therapeutics*, 159, 56–65. <https://doi.org/10.1016/j.pharmthera.2016.01.008>

Guy, A. J., Nath, J., Cobbold, M., Ludwig, C., Tennant, D. A., Inston, N. G., & Ready, A. R. (2015). Metabolomic analysis of perfusate during hypothermic machine perfusion of human cadaveric kidneys. *Transplantation*, 99(4), 754–759. <https://doi.org/10.1097/TP.0000000000000398>

Hauet, T., Baumert, H., Gibelin, H., Hameury, F., Goujon, J. M., Carretier, M., & Eugene, M. (2000). Noninvasive monitoring of citrate, acetate, lactate, and renal medullary osmolyte excretion in urine as biomarkers of exposure to ischemic reperfusion injury. *Cryobiology*, 41(4), 280–291. <https://doi.org/10.1006/cryo.2000.2291>

Hrydziusko, O., Perera, M. T. P. R., Laing, R., Kirwan, J., Silva, M. A., Richards, D. A., Murphy, N., Mirza, D. F., & Viant, M. R. (2016). Mass Spectrometry based metabolomics comparison of liver grafts from donors after circulatory death (DCD) and donors after brain death (DBD) used in human orthotopic liver transplantation. *PLoS ONE*, 11(11), e0165884. <https://doi.org/10.1371/journal.pone.0165884>

Humphries, T., Vesey, D., Galloway, G., Gobe, G., Francis, R. (2023). Identifying disease progression in chronic kidney disease using proton magnetic resonance spectroscopy. *Progress in Nuclear Magnetic Resonance Spectroscopy*, 134-135, 52–64 <https://doi.org/10.1016/j.pnmrs.2023.04.001>

Iwamoto, H., Okihara, M., Akashi, I., Kihara, Y., Konno, O., Kawachi, S., Sunamura, M., Sugimoto, M. (2022). Metabolomic profiling of plasma, urine, and saliva of kidney transplantation recipients. *International journal of molecular sciences*, 23(22), 13938 <https://doi.org/10.3390/ijms232213938>

Jacob, M., Lopata, A. L., Dasouki, M., & Abdel Rahman, A. M. (2019). Metabolomics toward personalized medicine. *Mass Spectrometry Reviews*, 38(3), 221–238. <https://doi.org/10.1002/mas.21548>

Jouret, F., Leenders, J., Poma, L., Defraigne, J.-O., Krzesinski, J.-M., & de Tullio, P. (2016). Nuclear magnetic resonance metabolomic profiling of mouse kidney, urine and serum following renal ischemia/reperfusion injury. *PLoS ONE*, 11(9), e0163021. <https://doi.org/10.1371/journal.pone.0163021>

Khbouz, B., Lallemand, F., Cirillo, A., Rowart, P., Legouis, D., Sounni, N. E., Noel, A., De Tullio, P., De Seigneux, S., & Jouret, F. (2022). Kidney-targeted irradiation triggers renal ischemic preconditioning in mice. *American Journal of Physiology-Renal Physiology*, 323(2), F198–F211. <https://doi.org/10.1152/ajprenal.00005.2022>

Koffman, G., & Gambaro, G. (2003). Renal transplantation from nonheart-beating donors: A review of the European experience. *Journal of Nephrology*, 16(3), 334–341.

Kurata, H., Fujii, T., Tsutsui, H., Katayama, T., Ohkita, M., Takaoka, M., Tsuruoka, N., Kiso, Y., Ohno, Y., Fujisawa, Y., Shokoji, T., Nishiyama, A., Abe, Y., & Matsumura, Y. (2006). Renoprotective effects of *l*-carnosine on ischemia/reperfusion-induced renal injury in rats. *Journal of Pharmacology and Experimental Therapeutics*, 319(2), 640–647. <https://doi.org/10.1124/jpet.106.110122>

Letertre, M. P. M., Giraudeau, P., & De Tullio, P. (2021). Nuclear magnetic resonance spectroscopy in clinical metabolomics and personalized medicine: Current challenges and perspectives. *Frontiers in Molecular Biosciences*, 8, 698337. <https://doi.org/10.3389/fmolb.2021.698337>

Lunyera, J., Diamantidis, C. J., Bosworth, H. B., Patel, U. D., Bain, J., Muehlbauer, M. J., Ilkayeva, O., Nguyen, M., Sharma, B., Ma, J. Z., Shah, S. H., & Scialla, J. J. (2022). Urine tricarboxylic acid cycle signatures of early-stage diabetic kidney disease. *Metabolomics*, 18(1), 5. <https://doi.org/10.1007/s11306-021-01858-4>

Mannon, R. B. (2018). Delayed graft function: The AKI of kidney transplantation. *Nephron*, 140(2), 94–98. <https://doi.org/10.1159/000491558>

Metzger, R. A., Delmonico, F. L., Feng, S., Port, F. K., Wynn, J. J., & Merion, R. M. (2003). Expanded criteria donors for kidney transplantation. *American Journal of Transplantation*, 3, 114–125. <https://doi.org/10.1034/j.1600-6143.3.s4.11.x>

Nath, J., Smith, T. B., Patel, K., Ebbs, S. R., Hollis, A., Tennant, D. A., Ludwig, C., & Ready, A. R. (2017). Metabolic differences between cold stored and machine perfused porcine kidneys: A ¹H NMR based study. *Cryobiology*, 74, 115–120. <https://doi.org/10.1016/j.cryobiol.2016.11.006>

Novitzky, T., Cooper, D. K. C., Morrell, D., & Isaacs, S. (1988). Change from aerobic to anaerobic metabolism after brain death and reversal following triiodothyronine therapy. *Transplantation*, 45(1), 32–36. <https://doi.org/10.1097/00007890-198801000-00008>

Peng, P., Ding, Z., He, Y., Zhang, J., Wang, X., & Yang, Z. (2019). Hypothermic machine perfusion versus static cold storage in deceased donor kidney transplantation: A systematic review and meta-analysis of randomized controlled trials. *Artificial Organs*, 43(5), 478–489. <https://doi.org/10.1111/aor.13364>

Ponticelli, C. (2014). Ischaemia-reperfusion injury: A major protagonist in kidney transplantation. *Nephrology Dialysis Transplantation*, 29(6), 1134–1140. <https://doi.org/10.1093/ndt/gft488>

Ponticelli, C., Reggiani, F., & Moroni, G. (2022). Delayed graft function in kidney transplant: Risk factors, consequences and prevention strategies. *Journal of Personalized Medicine*, 12(10), 1557. <https://doi.org/10.3390/jpm12101557>

Rao, P. S., Schaubel, D. E., Guidinger, M. K., Andreoni, K. A., Wolfe, R. A., Merion, R. M., Port, F. K., & Sung, R. S. (2009). A comprehensive risk quantification score for deceased donor kidneys: The kidney donor risk index. *Transplantation*, 88(2), 231–236. <https://doi.org/10.1097/TP.0b013e3181ac620b>

Reese, P. P., Aubert, O., Naesens, M., Huang, E., Potluri, V., Kuypers, D., Bouquegneau, A., Divard, G., Raynaud, M., Bouatou, Y., Vo, A., Glotz, D., Legendre, C., Lefaucheur, C., Jordan, S., Empana, J.-P., Jouven, X., & Loupy, A. (2021). Assessment of the utility of kidney histology as a basis for discarding organs in the United States: A comparison of international transplant practices and outcomes. *Journal of the American Society of Nephrology*, 32(2), 397–409. <https://doi.org/10.1681/ASN.2020040464>

Robert, R., Guilhot, J., Pinsard, M., Longeard, P.-L., Jacob, J.-P., Gissot, V., Hauet, T., & Seguin, F. (2010). A pair analysis of the delayed graft function in kidney recipient: The critical role of the donor. *Journal of Critical Care*, 25(4), 582–590. <https://doi.org/10.1016/j.jcrc.2010.02.011>

Rodriguez-Nino, A., Pastene, D. O., Post, A., Said, M. Y., Gomes-Neto, A. W., Kieneker, L. M., Heiner-Fokkema, M. R., Esatbeyoglu, T., Rimbach, G., Schnuelle, P., Yard, B. A., & Bakker, S. J. L. (2021). Urinary carnosinase-1 excretion is associated with urinary carnosine depletion and risk of graft failure in kidney transplant recipients: Results of the transplantlines cohort study. *Antioxidants*, 10(7), 1102. <https://doi.org/10.3390/antiox10071102>

Saat, T. C., Van Den Engel, S., Bijman-Lachger, W., Korevaar, S. S., Hoogduijn, M. J., IJzermans, J. N. M., & De Bruin, R. W. F. (2016). Fate and effect of intravenously infused mesenchymal stem cells in a mouse model of hepatic ischemia reperfusion injury and resection. *Stem Cells International*, 2016, 1–9. <https://doi.org/10.1155/2016/5761487>

Salvadori, M., Rosso, G., & Bertoni, E. (2015). Update on ischemiareperfusion injury in kidney transplantation: Pathogenesis and treatment. *World Journal of Transplantation*, 5(2), 52. <https://doi.org/10.5500/wjt.v5.i2.52>

Siedlecki, A., Irish, W., & Brennan, D. C. (2011). Delayed graft function in the kidney transplant. *American Journal of Transplantation*, 11(11), 2279–2296. <https://doi.org/10.1111/j.1600-6143.2011.03754.x>

Soussi, D., Rod, X., Thuillier, R., Leblanc, S., Goujon, J.-M., Barrou, B., Hauet, T., & Kerforne, T. (2019). Preclinical modeling of DCD class III donation: Paving the way for the increased use of this challenging donor type. *BioMed Research International*, 2019, 5924101. <https://doi.org/10.1155/2019/5924101>

van Der Hoeven, J. A. B., Molema, G., Ter Horst, G. J., Freund, R. L., Wiersema, J., van Schilfgaarde, R., Leuvenink, H. G. D., & Ploeg, R. J. (2003). Relationship between duration of brain death and hemodynamic (in)stability on progressive dysfunction and increased immunologic activation of donor kidneys. *Kidney International*, 64(5), 1874–1882. <https://doi.org/10.1046/j.1523-1755.2003.00272.x>

Wang, Z., Durai, P., & Tiong, H. Y. (2020). Expanded criteria donors in deceased donor kidney transplantation—An Asian perspective. *Indian Journal of Urology: IJU: Journal of the Urological Society of India*, 36(2), 89–94. https://doi.org/10.4103/iju.IJU_269_19

Wishart, D. S. (2006). Metabolomics in monitoring kidney transplants. *Current Opinion in Nephrology and Hypertension*, 15(6) 637–642. <https://doi.org/10.1097/01.mnh.0000247499.64291.52>

Wong, G., Teixeira-Pinto, A., Chapman, J. R., Craig, J. C., Pleass, H., McDonald, S., & Lim, W. H. (2017). The impact of total ischemic time, donor age and the pathway of donor death on graft outcomes after deceased donor kidney transplantation. *Transplantation*, 101(6), 1152–1158. <https://doi.org/10.1097/TP.0000000000001351>